Journal of Structural Geology, Vol. 9, No. 3, pp. 299 to 311, 1987
Printed in Great Britain

0191-8141/87 $03.00 + 0.00
Pergamon Journals Ltd.

Microstructure, *c*-axis pattern, microstrain and kinematics of some *S–C* mylonites in Grenville gneiss

NICHOLAS CULSHAW

Geological Survey of Canada*

(*Received* 17 *June* 1985; *accepted in revised form* 17 *September* 1986)

Abstract—In a major tectonic zone late extension related *S–C* mylonites locally overprint the predominant coarser quartz microstructures, which are related to earlier thrusting. Some of the *S–C* mylonites display a microstructural evolution which began with the formation of deformation bands in the coarser pre-existing microstructure and continued with the formation of asymmetric quartz microfoliations, either by continued formation of deformation bands or fine new grains oblique to the deformation band boundaries. The orientation of boudinaged and passively reoriented rutile needles show that (i) the formation of deformation bands was preceded and accompanied by the accumulation of strain; (ii) that the deformation bands and oblique microfoliation which formed directly from them lie close to the finite stretching direction; whereas (iii) other microfoliations form oblique to deformation bands and extended rutile needles near the probable instantaneous stretching direction. The latter are therefore interpreted to be strain insensitive, steady-state foliations. The crystallographic preferred orientation of the original deformation bands appears to determine that of the microfoliations, the two types of microfoliations showing distinct but related patterns. The element common to both types is the presence of two maxima near *Y* in a *YZ* girdle—a feature inherited from the deformation bands, which were formed in the initial stages of shortening of the aggregate, favourably disposing it for rhomb slip and providing nucleation sites for subsequent recrystallization.

The data confirm that, despite the fact that a variety of microstructures and crystallographic microfabrics result from recrystallization processes, kinematic information is usually recoverable from the crystallographic microfabrics owing to the primacy of intracrystalline slip processes.

INTRODUCTION

THIS PAPER deals with aspects of the development of oblique grain shape microfabrics (*LS2*) defined by the preferred alignment of elongate recrystallized quartz grains. These oblique microfabrics form the *S* component of *S–C* mylonites (Lister & Snoke 1984) which occur sporadically within a zone of deformed plutonic and supracrustal gneiss underlying the south western end of the base of the Central Metasedimentary Belt within the Grenville Province of the Canadian Shield (Fig. 1).

Evidence is presented to show that most of the oblique microfabrics originate from deformation bands which formed in a much coarser earlier microstructure in a manner such that the deformation bands themselves become new grains or provide the sites for a finer recrystallization. Furthermore the *c*-axis orientation of the oblique microfabrics appears to be influenced by the orientations present in the deformation bands such that the two maxima are symmetrically disposed to *Y* within a *YZ* girdle—a feature common to several of the tectonites which may reflect the original kink-like geometry of the deformation bands. Thus the *c*-axis patterns are not only the product of available glide systems, finite strain and kinematic framework (Lister *et al.* 1978, Lister & Paterson 1979, Lister & Hobbs 1980) but also to a significant extent they are recrystallization microfabrics. Finally, the preferred orientation of rutile inclusions shows that considerable plastic strain preceded and accompanied the formation of the deformation bands and that the oblique fabrics, where formed directly from a deformation band without finer recrystallization, lie parallel to the finite stretching direction, or, where a finer recrystallization has taken place, appears to lie near the instantaneous stretching direction, as in the case of the postulated steady-state foliations of Means (1981).

An important general point is that despite the quite dissimilar microstructures and crystallographic fabrics produced in quartz by the *LS2* event, the subject of this study, and the probably higher grade *LS1* event (Culshaw & Fyson 1984), the kinematic record remains legible in both. This is presumably because of the first order importance, compared to other effects, of finite strain, kinematic framework and available slip systems in determining crystallographic fabrics.

Geological setting

The zone of deformed gneiss which is host to the *S–C* mylonites is a wide zone of northwest directed ductile thrusting (Culshaw *et al.* 1983, Hanmer & Ciesielski 1984) parallel to a ubiquitous stretching lineation which plunges gently to the southeast. This thrusting event is recorded microscopically by the most widespread quartz microstructures (*LS1*) which comprise polycrystalline ribbons of relatively coarse quartz in granitoids and

* Present address: Dalhousie University, Department of Geology, Halifax, Nova Scotia, Canada, B3H 3J5.

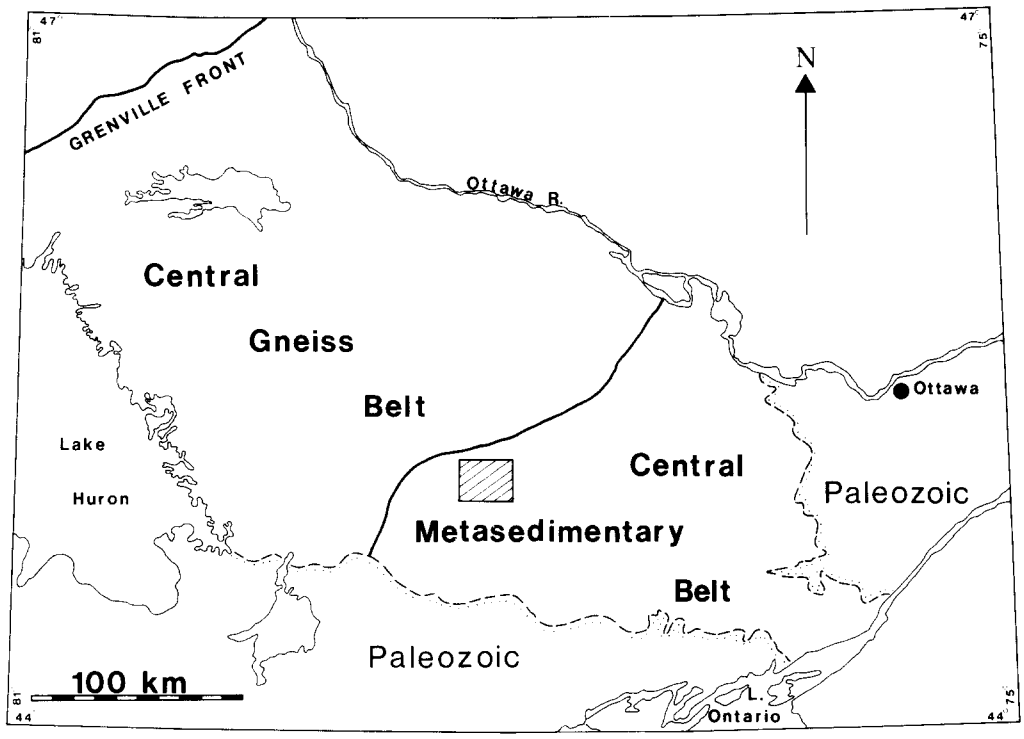

Fig. 1. Map showing location of sample area (cross-hatched). Two major divisions of the Grenville province within Ontario (southwest of Ottawa River) are shown. The Central Metasedimentary Belt is overthrust onto the Central Gneiss belt along a wide, shallow-dipping, zone of ductile deformation, which contains the sample area.

exaggerated grain-growth microstructures in quartzites (Culshaw & Fyson 1984). The *S–C* mylonites (*LS2*) cannot be mapped in the field since they are generally only microscopically visible but samples with this microstructure are most commonly collected within the zones of macroscopically strongest deformation, indicated by the degree of flagginess and grain size refinement of quartzofeldspathic rocks. Their total volume is probably only a few per cent of the whole deformed zone.

The *S–C* mylonites (*LS2*) are clearly later than the main phase tectonites (*LS1*) since the finer microstructures replace the coarser and rare *S–C* mylonites which dip northwest and transpose *LS1* tectonites. It is not possible to be precise about the temperature conditions of formation of *LS2*, since diagnostic mineral assemblages are scarce. A single occurrence of biotite–muscovite in association with *LS2*-muscovite is absent in main phase schists and the sporadic occurrence of green biotite replacing brown varieties in the granitoids suggests a temperature regime somewhat lower than the main phase, although still possibly broadly contemporaneous. Chesworth (1971) suggested that the peak conditions of metamorphism for the area lay within the limits of 3.5–7 kb and 580–700°C.

In most of the *S–C* (*LS2*) tectonites the *c*-plane lies with *S1* and both the obliquity of *S2* and the relation of the *LS2* *c*-axis pattern to *S1* and *S2* imply dip–slip parallel to *L1* (Fig. 2). For the single sample from a northwest dipping zone the same criteria also imply dip–slip. Overall, therefore, the *LS2* fabrics imply a period of extension following the main phase (*LS1*) thrusting.

DEFORMATION BANDS AND THE INITIATION OF THE OBLIQUE FABRIC

The role played by the formation of deformation bands in the development of the oblique fabric is displayed in tectonites where *LS2* recrystallization is

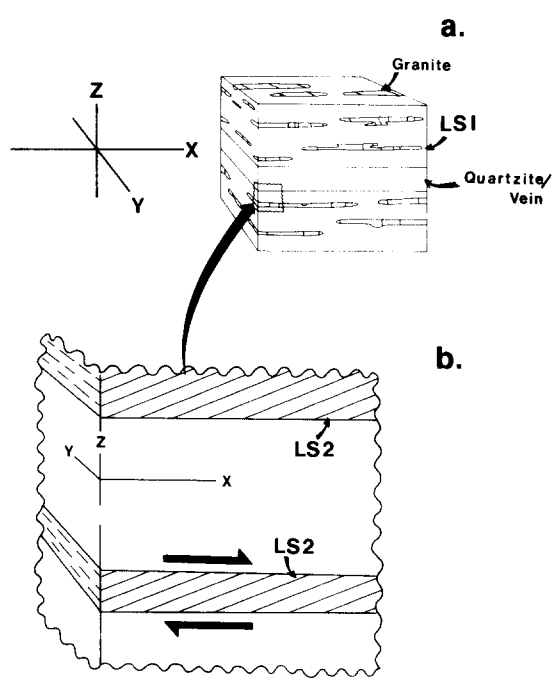

Fig. 2. Relations between macroscopic *LS1* fabric and microscopic *LS2* fabric. *LS1* structural co-ordinates are defined by the shape of quartz blades in the *LS* granite. *LS2* microfoliations have shear-plane within *S1* (*XY*) and shear direction parallel to *L1* (*X*).

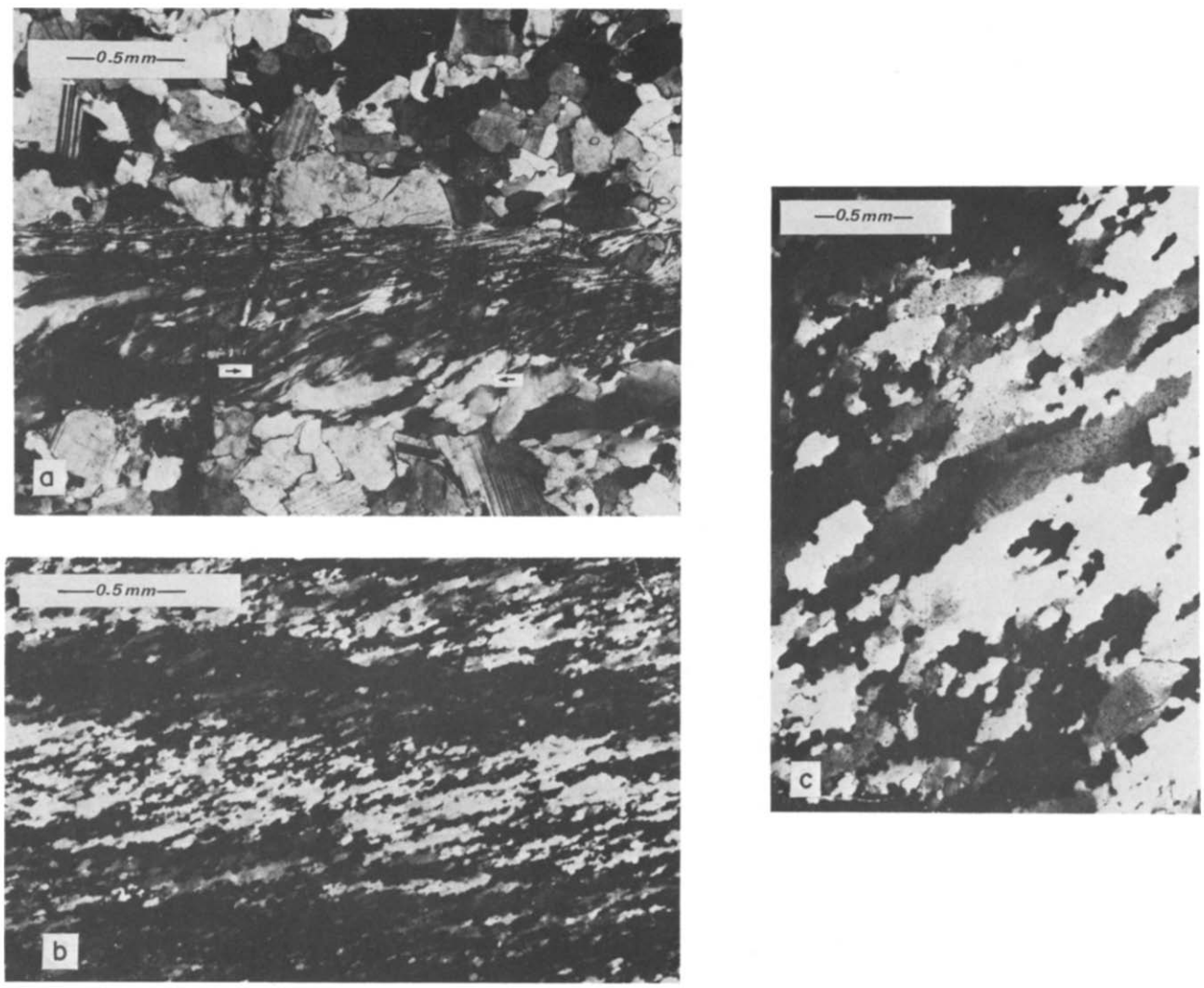

Fig. 3. Main types of asymmetric *LS2* quartz microfoliations. All are *XZ* sections viewed toward the northeast (*X* horizontal, downdip to right). (a) *LS1* quartz ribbon in foliated granite is extensively replaced by deformation band parallel microfoliation; data shown in Fig. 5(a) is from area of deformation band development which lies along the lower part of the ribbon indicated by arrows; *c*-axis for this sample shown in Fig. 6(a,i). (b) In a concordant quartz vein deformation band non-parallel microfoliations lie oblique to recrystallized deformation bands, marked now by extinction banding (*c*-axis for this sample shown in Fig. 6b, i). (c) In a quartzite the large grains are inferred to be developed from deformation bands which formed in a very coarse exaggerated grain growth microstructure (data from this sample shown in Figs. 5d and 7c and *c*-axis shown in Fig. 6a, ii).

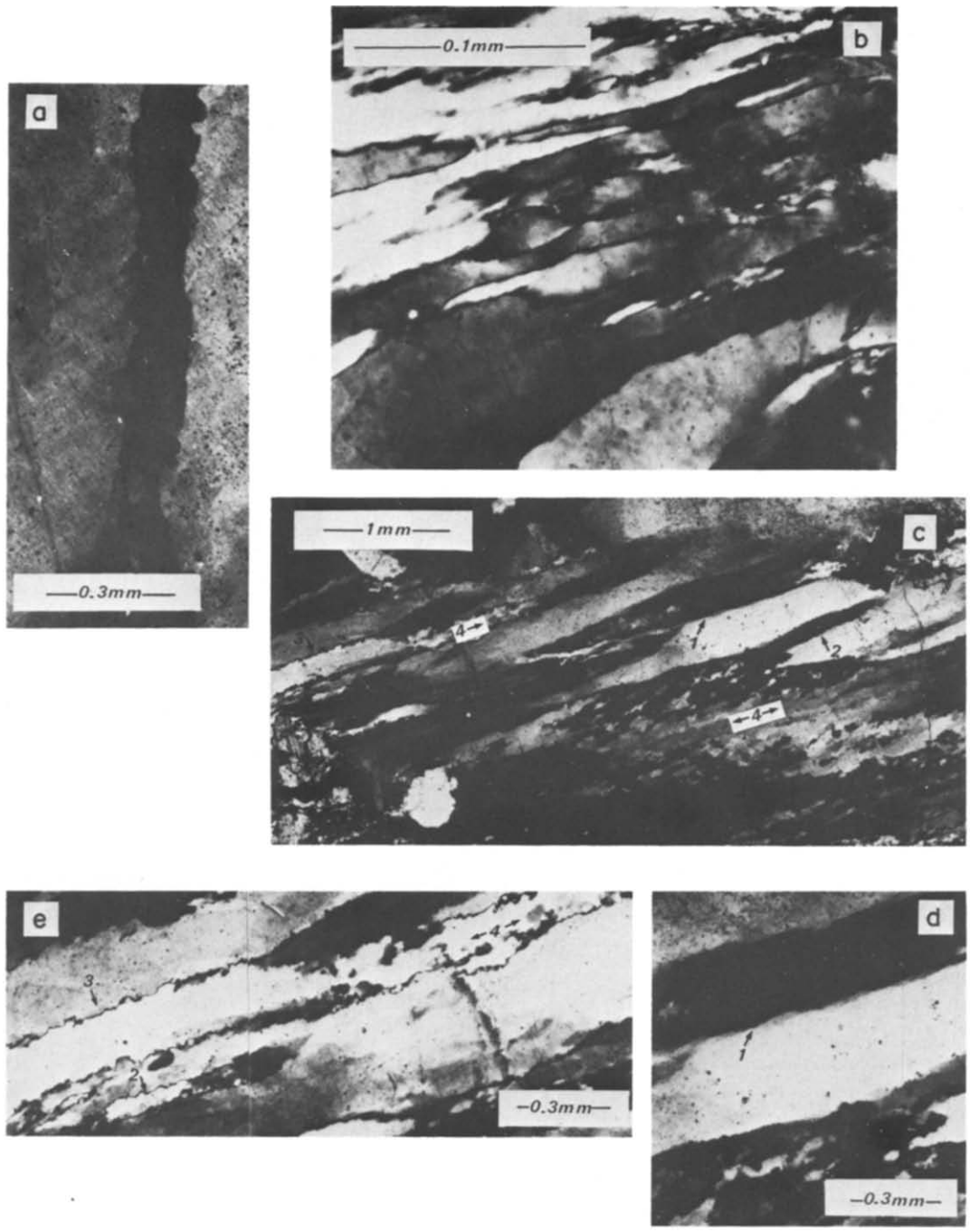

Fig. 4. Details of development of *LS2* microfoliations from deformation bands. (a) Deformation band with variable irregular boundary formed within coarse quartz inherited from pre-existing exaggerated grain growth microstructure; quartzite with assumed deformation band parallel microfoliation. (b) Typical aspect of deformation band parallel microfoliation in foliated granite; a portion of an *LS2* quartz ribbon of single original orientation is traversed by increasingly thinner deformation bands; note relatively smooth boundaries and low misorientations. (c), (d) & (e) Formation of deformation band non-parallel microfoliations. (c) At the margin of a concordant quartz vein an area of quartz of single original orientation is subdivided by numerous transverse deformation bands; boundary morphology ranges from smooth, through irregular, to irregular-asymmetric (both with and without new grains) while some deformation bands display fine recrystallization. In (c), (d) & (e) details of deformation bands shown by arrows: 1, smooth boundary; 2, irregular boundary; 3, asymmetric irregularities (note sub-grains within some protuberances); 4, fine recrystallization in deformation band interior. Data in Fig. 5(e) and Table 1 are from area of deformation band partially illustrated in upper part of (b). All *XZ* sections (*X* horizontal, except in a) viewed to northeast.

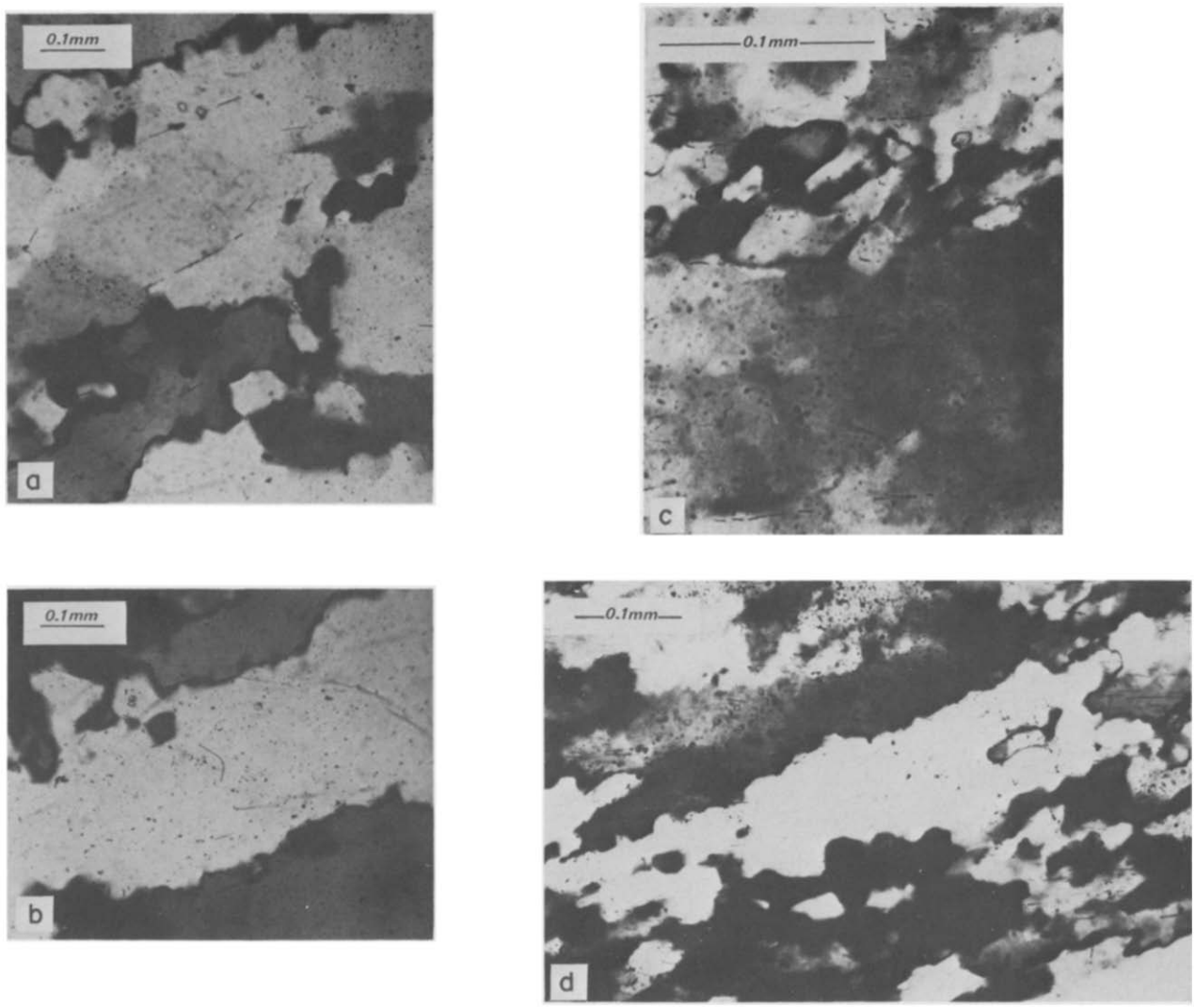

Fig. 8. Relations of rutile needles and *LS2* asymmetric microfoliations. (a)–(b) From concordant quartz vein with microfoliation inferred to be deformation band-parallel; rutile lies parallel to *LS2* trace in (a), while rutile lying at a high angle to *LS2* trace is bent in (b) (data from this sample also shown in Fig. 7a and b and *c*-axis shown in Fig. 6a, iii). (c)–(d) Deformation band-non-parallel microfoliations; (c) extended rutile needles lie parallel to deformation band boundary but transverse to *LS2* grains (from quartz vein in northwest dipping granite mylonite, data also in Fig. 7d and *c*-axes shown in Fig. 6b, iii); (d) rutile needles transect *LS2* grains in concordant quartz veins (data also in Fig. 7e) and *c*-axis data shown in Fig. 6(b,i). All in *XZ* sections (*X* horizontal) viewed toward northeast, except (c) which is viewed toward southwest and dips to northwest.

incomplete. Two principal modes of development are present, both begin with the formation of deformation bands which partly define the oblique fabric (Figs. 3 and 4). In the first case, displayed by a foliated granite, *LS2* is formed by the progressive multiplication of successive thinner deformation bands, which at the same time gain a strong *c*-axis preferred orientation and are passively reoriented toward the *c*-plane (Figs. 3a and 4b). The grains parallel to deformation bands are relatively straight sided ribbons (Figs. 3a and 4b), although there is evidence from grain size, *c*-axis orientation and rutile inclusion data (see below) that, in some samples of quartzites and quartz veins, foliations formed of large grains with very irregular boundaries are produced in the same way (Figs. 3c and 4a).

In the second case, recrystallization occurs both within and at the boundaries of the deformation bands and is markedly oblique to the deformation band boundary (Figs. 3b and 4c–e). Grains formed in this way are of lower aspect ratio and much finer than the deformation band parallel grains and have irregular lobate boundaries (Fig. 3b). In detail, the boundaries of these deformation bands vary from quite straight to irregular (Fig. 4c–e). This type of microfoliation closely resembles that often illustrated in recent literature (e.g. Lister & Snoke 1984).

A third type of microstructure, not illustrated here, does not show any relationship between deformation bands and oblique foliation. The oblique foliation is fine grained and resembles the fine recrystallized grains of the deformation band oblique foliations.

GEOMETRY OF DEFORMATION BANDS

A common feature of all the deformation bands is that the intersections of the basal planes of nearest-neighbour bands lie in or near the trace on the *XY* plane of the oblique fabric (Fig. 5). This suggests that the deformation bands have kink-like geometry with the axis of rotation (the intersection of nearest-neighbour's basal planes) lying in the kink-band boundary (deformation band boundary) (Christie *et al.* 1964). For this geometry the slip plane must be the basal plane.

This relationship is best displayed in the specimen with deformation band parallel foliation (Fig.5a–c). In a partly recrystallized area of this microstructure both relatively broad deformation bands and thinner bands, characteristic of the oblique fabric, display parallelism of nearest-neighbour basal plane intersections to band boundaries (*LS2* trace) (Figs. 3a and 5a). In fact most of these *LS2* ribbon grains show the same kink-like relationship of nearest-neighbour grains throughout the microstructure (Fig. 5b–c). Thus, in this type of microstructure, this relationship is found at all stages of microstructural development. A similar geometry is shown by deformation bands in the microstructure with the deformation band non-parallel foliation (Fig. 5e). It differs from the deformation band parallel foliation in that the measured misorientation between bands is relatively limited at the onset of recrystallization, which takes place both at the deformation band boundaries and within the bands producing relatively fine grains which define the foliation (Fig. 4c–e). The boundaries of bands in this specimen evolve morphologically during the initiation of the recrystallization. The variation is from smooth, planar boundaries, through boundaries with increasing proportions of irregular bulbous segments, to boundaries with protuberances oriented parallel to *LS2* and both sub- and new grains in this orientation (Fig. 4c–e). This change is accompanied, in this small sample, by an increase in the angle between basal planes of neighbouring bands (Table 1). These features indicate a progressive evolution of deformation band boundaries and reorientation of bands prior to and during recrystallization.

Table 1. Angle (θ) between basal planes of neighbouring deformation bands

Morphology of deformation band boundary	*N*	Mean θ	S.D.	Range
Smooth	7	13°	2°	10–17°
With bulbous segments	29	18°	9°	7–48°
With bulbous segments parallel to *LS2*	12	26°	8°	12–38°

This nearest-neighbour geometry is also displayed in the microstructures associated with grains which are much larger than in the deformation band non-parallel fabrics (although a secondary population of fine equant grains is apparent) but have irregular corrugated boundaries, unlike the other ribbon-like deformation band-parallel fabrics (Fig. 3c). Although direct evidence of *LS2* formation from deformation bands is rarely present in this type (Fig. 4a), the preservation of kink-like nearest-neighbour geometry (Fig. 5d) in the larger grains, together with the large size of some of the grains (Fig. 3c), is interpreted as indirect evidence of descent of the grains from deformation bands by some mechanism of grain boundary motion. The parent deformation bands having formed within the pre-existing, much coarser, exaggerated grain growth microstructure (Fig. 4a).

DEFORMATION BANDS AND *c*-AXIS PATTERNS

There is a correlation between the type of oblique microfabric, classified according to its interpreted original relationship to deformation bands, and *c*-axis pattern. The samples with proven and inferred deformation band parallel fabrics show well developed paired maxima lying within a girdle perpendicular to *S1* (Fig. 6a, i–iii). The fine grained, more profusely recrystallized deformation non-parallel fabrics show a somewhat different pattern in which these maxima are accompanied by others within the *YZ* girdles (Fig. 6b, i–iii). By way of contrast, those foliations with no obvious relation to deformation bands do not show paired maxima near *Y* (Fig. 6c, i–ii). This correlation suggests a link between

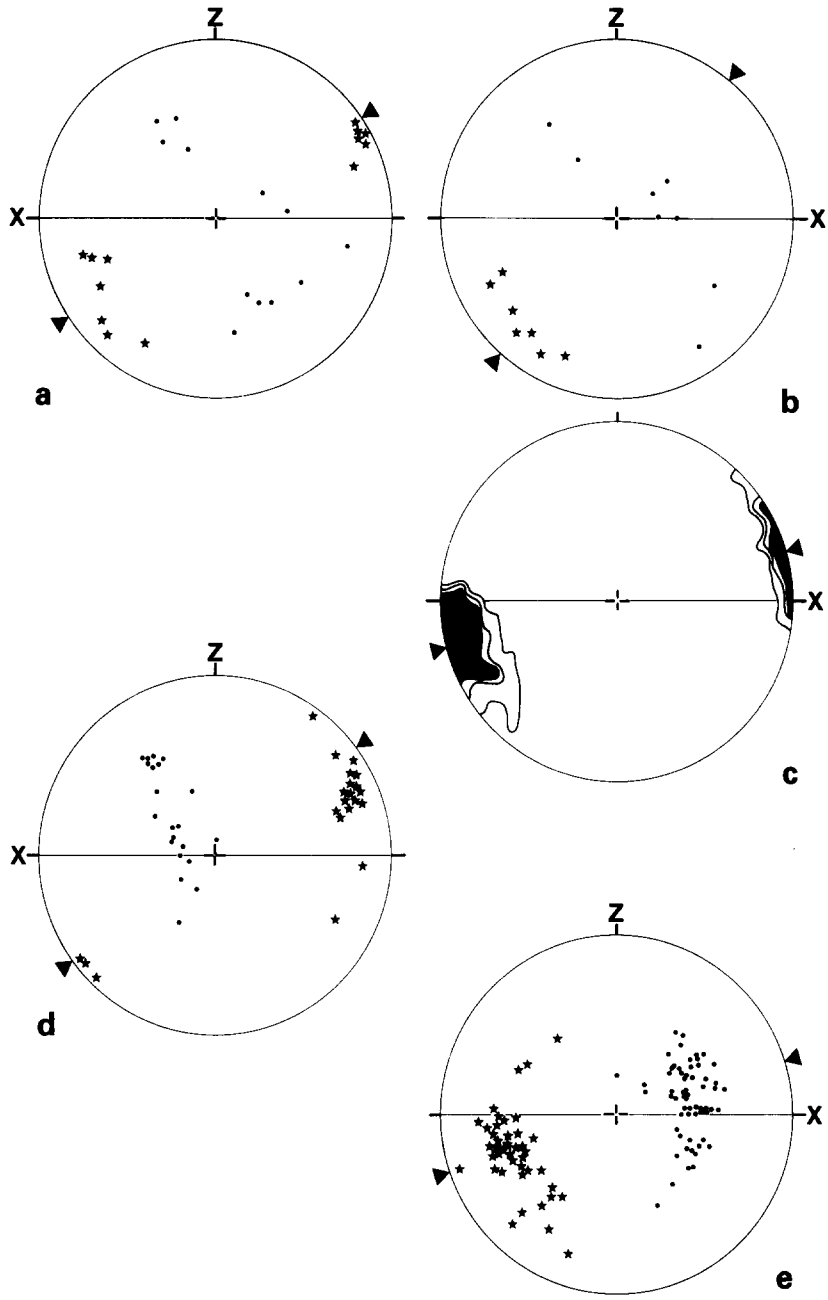

Fig. 5. Orientation of axes of rotation (intersection of basal planes) of both nearest-neighbour deformation bands and *LS2* grains. Intersections of basal planes (stars), poles to basal planes (solid circles) and *LS2* trace (solid triangle). In (c) the distribution of intersections is contoured at 3, 5 and 6%/1% area, $N = 200$. Measurements are made from (a) the area of deformation band and adjacent ribbons in the deformation band parallel type microfoliation shown in Fig. 3(a), (b) from a comparable microdomain in the same section, (c) from nearest-neighbour ribbon grains in the same sample, (d) from large grains in the inferred deformation band parallel type and (e) from deformation bands from the area illustrated in Fig. 4(c)–(e) in a sample with the deformation band non-parallel microfoliations.

microstructural development and *c*-axis pattern, such that the mode of recrystallization is important not only in forming the microstructure but also has an influence on the type of crystallographic preferred orientation attained.

This link is apparent in microstructural data from the specimen with the deformation band parallel foliation and best developed double maxima (Figs. 3a, 4b, 5a–c and 6a, i). As outlined in the previous section, deformation bands in this sample evolve into the oblique quartz ribbons (*LS2*) while the kink-like relation of nearest-neighbour bands and ribbons is preserved (Fig. 5a–c). Since this kink-like relation holds for all the nearest-neighbours measured, such that the kink-axis (intersection of nearest-neighbour basal planes) lies close to the oblique foliation trace (*LS2*) (Fig. 5c), then the gross *c*-axis pattern (Fig. 6a, i) reflects the geometry of nearest-neighbour deformation bands and ribbons (*LS2*). In the case of the deformation band non-parallel foliations deformation bands play a comparable role, as indicated by nearest-neighbour deformation band geometry (Fig. 5e) and *c*-axis patterns (Fig. 6b, i–iii). However, both the profuseness of fine-grained recrystallization and the presence of other maxima in the girdle

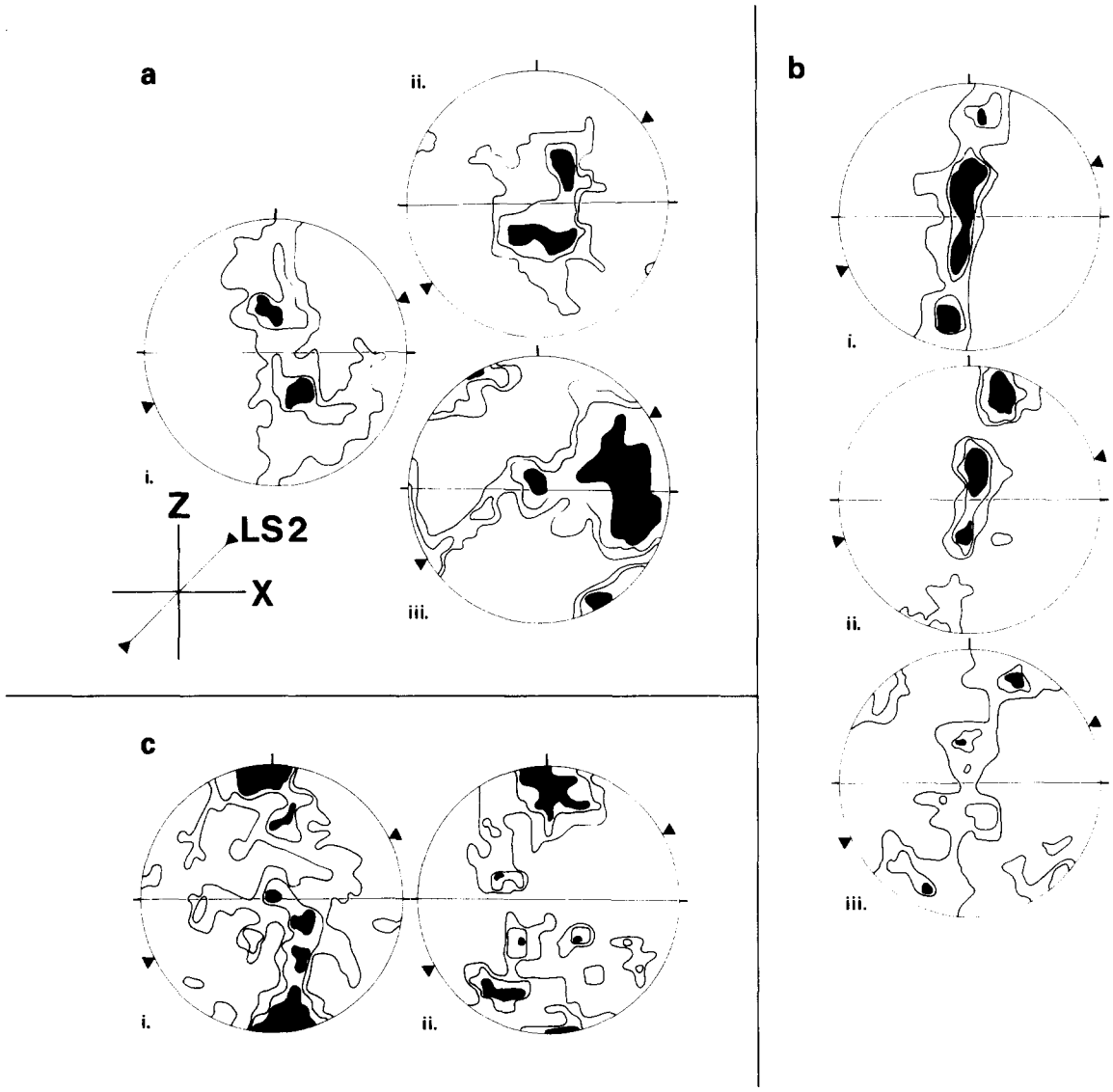

Fig. 6. *c*-axis orientations in *LS2* tectonites. All data measured in *XZ* plane of *LS1*, with dextral shear parallel to *L1* (*X*) present in all cases. Three microstructural types represented: (a) deformation band-parallel microfoliation, proven (i), inferred (ii, iii); (b) deformation band parallel microfoliations; (c) microfoliations with no demonstrable relationship to deformation bands. All contours at 1, 3 and 5% except (b,ii) at 1, 4 and 8% and (c,i) at 1, 2 and 3%; $N = 200$ in all, except (b,ii), in which $N = 100$.

(Fig. 6b, i–iii) suggest that nearest-neighbour deformation band geometry plays a more indirect role in determining the overall lattice preferred orientation of these samples. Instead, it appears that the formation of deformation bands is quickly superseded by fine grained recrystallization oblique to deformation bands (Figs. 3b and 4c–e). The role of the deformation bands in this case is to provide a host orientation for the finer recrystallization to which it is related by a geometrical law distinct from that which relates neighbouring deformation bands (Bell & Etheridge 1976, White 1976). Thus the deformation band geometry in the overall *c*-axis pattern is diluted, producing other maxima in the *YZ* girdle (Fig. 6b, i–iii). Overall these data imply that evolution of microstructure and *c*-axis pattern is closely interlinked; especially that the development of two maxima near *Y* is associated with deformation band formation and that the mode of recrystallization is also a factor in influencing details of the *c*-axis pattern.

RUTILE INCLUSIONS AND OBLIQUE FABRICS

Rutile inclusions have been used previously to gain strain information in quartz-rich rocks (Mitra 1976, Mitra & Tullis 1979). In the present case rutile inclusions although not present in all the samples are present in all the inferred microstructural types and the relation between finite stretching direction and oblique foliations is clearly displayed. Rutile is absent from the sample in which the development of the deformation band parallel fabrics can be best documented, but two samples which have been inferred indirectly to have this fabric on the grounds of microstructure (Fig. 3c) and *c*-axis patterns (Figs. 6a, ii–iii) show behaviour of rutile needles consistent with this interpretation. In one of these samples the rutile which is contained within an irregular patch of unrecrystallized quartz shows a quasi-uniform distribution (Fig. 7a) while within a neighbouring domain of oblique *LS2* grains the needles have a preferred orienta-

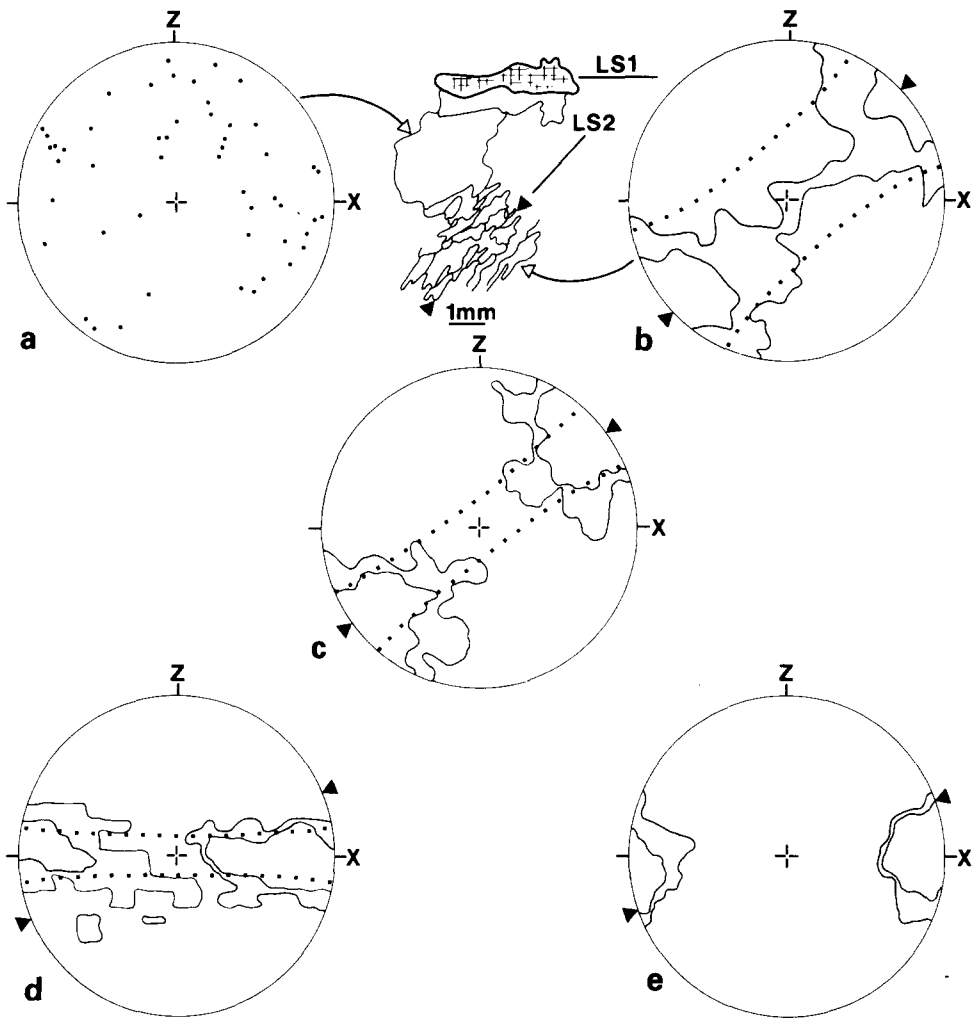

Fig. 7. Orientation of rutile needles in *LS2* tectonites. (a)–(c) From inferred deformation band-parallel microfoliations; (d)–(e) from deformation band non-parallel microfoliations; solid triangle, trace of *LS2* microfoliation. Field of contracted needles separated from field of extended needles by line of solid squares. Contours at 1 and 3%/1% area in (b)–(e); $N = 200$ in (b), 150 in (c) and 100 in (d) and (e). Orientations are displayed for unrecrystallized and undeformed quartz (a) in quartz vein with inferred deformation band parallel microfoliation.

tion parallel to *LS2* (Fig. 7b). Many of the needles aligned parallel to *LS2* are boudinaged and display elongations of 20–30% while needles lying at a high angle to the oblique foliation may be bent (Fig. 8a,b). Similar features are present in the quartzite, which displays kink-band like geometry of nearest-neighbour grains (Figs. 3c and 5d), and in both these examples a sufficient number of bent and folded rutile needles are preserved to delineate fields of folded and extended needles (Fig. 7b,c). These boudinaged rutile needles are aligned parallel to *LS2* and display 10–20% elongations. It follows that in samples with inferred deformation band parallel foliations both the finite extension direction, deduced from the orientation of the rutile needles, and the oblique *LS2* foliations are closely aligned.

The relation between rutile needles and oblique foliations is significantly different in samples with deformation band non-parallel foliations. In both samples which have both deformation bands and the fine oblique recrystallization, rutile is often boudinaged and aligned parallel to the deformation band boundaries (Figs. 7d and 8c). In one case, as in the inferred deformation band parallel sample, fields of folded and extended needles may be delineated (Fig. 7d), the field of extension locally coinciding with the trace of the deformation bands. In both samples, the fine oblique *LS2* recrystallized foliation transects the rutile needles both at deformation-band boundaries and within completely recrystallized domains (Figs. 7d,e and 8c,d). The values of elongation measured from boudinaged rutiles in these samples are two to three times larger within the recrystallized domains than within the deformation bands. In one of these examples (Figs. 7e and 8d) a field of contraction cannot be delineated and needles are not present in unrecrystallized quartz without deformation bands. The needles in this case do not record the whole strain history and seem to have been precipitated sub-parallel to an active slip-plane during the evolution of the deformation bands. In microstructural types in which deformation bands did not play any role in influencing either the development of the oblique fabrics or the *c*-axis pattern (Fig. 6c i,iii), rutile is transected by the oblique foliation

in a manner similar to that in the deformation band non-parallel fine grained foliations.

Several conclusions follow directly from these observations. Firstly, support is given for the inference that some oblique fabrics are deformation band parallel by the alignment of extended rutile, both parallel to these foliations and parallel to deformation bands in deformation-band non-parallel tectonites. Secondly, significant strain must take place in deformation bands before recrystallization, since boudinage and alignment appears to be accompanied by an increase in strain. Finally, both the deformation band parallel foliation and the deformation bands appear to passively track the finite extension direction but the fine deformation band oblique foliation lies in a direction more akin to that expected for the instantaneous stretching direction in a simple shear regime and shows no discernible strain sensitivity.

DISCUSSION

The microstructural history of most of these *S–C* mylonites is marked by the early development of deformation bands sub-parallel to the future oblique foliation direction. The appearance of deformation bands early in microstructural development has been observed in metals by many authors, where they may both act as loci of recrystallization and determine the lattice preferred orientation of the products of recrystallization (Walter & Koch 1963, Dillamore *et al.* 1972, Doherty 1974, Inokuti & Doherty 1978). Their presence in the microstructural development of a wide variety of minerals is also well documented (e.g. Hobbs 1968, Etheridge & Hobbs 1974, McClay & Atkinson 1977, White 1977, Tungatt & Humphreys 1981) although specific mention of them determining the lattice preferred orientation of recrystallization is more rare (e.g. White 1976, Bell & Etheridge 1976). The origin by kinking of deformation bands was recognized in early experimental studies of quartz (Christie *et al.* 1964) and a similar origin for grains which host oblique microfoliations has been suggested by some authors (Lister & Snoke 1984).

In the present examples both the rutile data and crystallographic preferred orientation of the deformation bands indicate that considerable plastic deformation is accomplished in the coarse parent microstructure before widespread recrystallization. Moreover the idea of a progressive evolution of the deformation bands before recrystallization is supported by the evidence for linked change in band boundary morphology and angle between neighbouring basal planes (Table 1). The deformation bands appear to form during this stage in response to flattening accomplished by kinking in a simple shear regime. Subsequent to the phase of deformation band formation the microstructures evolve along different routes.

In the ribbon-grained deformation band parallel texture (Fig. 3a) the rate of band formation was high. Thus recrystallization was by band proliferation, forming the characteristic very strong double maxima of *c*-axes and disposing the aggregate for easy rhomb slip (Schmid 1983). Bands are passively rotated toward the slip-plane, demonstrating that this is a strain-sensitive, non-steady state fabric in the sense of Means (1981).

The rate of deformation band formation was clearly lower in the samples characterized by large grains with sutured boundaries which are inferred to be deformation band parallel (Fig. 3c). The irregular grain boundaries imply boundary mobility and we may postulate that deformation band boundaries became high angle boundaries as has been documented in a variety of metals and minerals (Hobbs 1968, Etheridge & Hobbs 1974, Bellier & Doherty 1977, McClay & Atkinson 1977, Cox & Etheridge 1984), and subsequently became mobile preserving a grain shape fabric normal to the overall shortening direction (Means 1983). Further alteration of this primitive geometry by continued recrystallization is shown by a comparison of Figs. 5(d) and 6(a,iii), which demonstrates that the population as a whole has a slip-plane which lies parallel to the macroscopic shear plane and not to the trace of *LS2*.

The most significant feature of the deformation band non-parallel foliations is that they transect the finite stretching direction delineated by the rutile needles (Figs. 7d,e and 8c,d) and that they lie in an orientation appropriate to that of the instantaneous stretching direction in a simple shear regime. This configuration, which is shared by fabrics in which deformation bands do not directly determine the oblique fabric, is directly comparable to that suggested by Means (1981) for a strain-insensitive, steady-state foliation. For this type of strain induced boundary migration (Poirier & Guillopé 1979) may be postulated for oblique protuberances at deformation band boundaries (Figs. 4e and 8c) and rotation recrystallization (Poirier & Guillopé 1979) within deformation band interiors (Fig. 4c–e). In this case the influence of band formation on *c*-axis orientation of the recrystallized grains would be more indirect than in the deformation band parallel sample, the role of host–daughter relationships being paramount, perhaps explaining the presence of other maxima in the *YZ c*-axis girdles.

In summary, good *c*-axis preferred orientations are formed in the *S–C* mylonites during dynamic recrystallization and in many cases the formation of deformation bands has been an important first step in the dynamic recrystallization of a pre-existing relatively coarse microstructure. These deformation bands appear to have an important influence on the subsequent development of microstructure and crystallographic fabric which may be manifested in several ways: (i) through repeated deformation band formation, (ii) through the mobilization of deformation band boundaries, either through motion of the entire boundary or a localized bulging, (iii) through rotation recrystallization within the deformation band, and (iv) through the imposition on the aggregate of a non-uniform initial orientation distribution which must affect crystallographic fabrics formed by intracrystalline slip (Lister & Hobbs 1980). A comparison of original

deformation band crystallographic preferred orientation (where preserved) and the final *c*-axis preferred orientations shows that these mechanisms preserve to a varied extent the deformation band orientations, although different combinations of recrystallization mechanisms result in variations in details of *c*-axis patterns. However, the most common element in all the patterns, two maxima near *Y* in a *YZ* girdle (a pattern disposing the aggregate for easy rhomb slip), is thus a direct descendant of processes operative during the initial period of deformation band formation. The relative orientations of deformation bands, asymmetric microfoliations and passively reoriented rutile needles show that deformation band formation is accompanied, and the formation of the microfoliations preceded, by considerable plastic deformation. There are two fundamentally different orientations of microfoliations with respect to the reoriented rutile needles: those which lie parallel to both deformation bands and rutile needles and those which lie at an angle to deformation bands and rutile needles in the attitude predicted for a strain insensitive steady state fabric. Samples with these two types of microfoliations also display the two varieties of *c*-axis pattern mentioned above. In a third type no relationship between deformation band formation and recrystallization was observed. Overall, the history of initial strain followed by probable steady-state dynamic recrystallization resembles that of dynamically recrystallized metals described by Sellars (1978).

The observations made here have a general import on the relative significance of processes contributing to the formation of quartz *c*-axis patterns and related microstructures. Above, it was noted that there were two quite different types of quartz crystallographic microfabrics and microstructures, *LS1* and *LS2*. *LS1* quartz ribbons, formed at upper amphibolite facies in foliated granites (Fig. 2), are comprised of several relatively coarse, blocky grains and *c*-axis patterns dominated by girdles with *Y* maxima (Culshaw & Fyson 1984). The grains which form the ribbons show interrelationships between *c*-axis orientation and aspect ratio such that a period of metadynamic oriented grain growth was postulated for their formation (Culshaw & Fyson 1984). The *LS2* quartz tectonites, as discussed above, show quite different microstructures, microstructural histories and *c*-axis patterns. However, despite the contrasting recrystallization histories, a kinematic record is legible in *c*-axis patterns of both types. This confirms that intracrystalline slip is a first order process in formation of quartz microfabrics and that therefore quartz tectonites formed under a wide variety of conditions may be optimistically approached for kinematic information provided care is taken to screen the effects of second order processes.

Acknowledgements—Many thanks to Simon Hanmer, Jack Henderson and Rein Tirrul who read an early version of the manuscript; and to an anonymous reviewer whose comments allowed a very great improvement. The author also acknowledges receipt of NSERC graduate scholarship, held at the University of Ottawa and an NSERC Visiting Fellowship at the Precambrian Division of the Geological Survey of Canada.

REFERENCES

Bell, T. H. & Etheridge, M. A. 1976. The deformation and recrystallization of quartz in a mylonite zone, central Australia. *Tectonophysics* **32**, 235–267.

Bellier, S. P. & Doherty, R. D. 1977. The structure of deformed aluminium—investigations with transmission Kossel diffraction. *Acta Metall.* **25**, 521–538.

Christie, J. M., Griggs, D. T. & Carter, N. L. 1964. Experimental evidence of basal slip in quartz. *Geology* **72**, 734–756.

Chesworth, W. 1971. Metamorphic conditions in a part of the Haliburton Highlands of Ontario. *Lithos* **4**, 219–229.

Cox, S. F. & Etheridge, M. A. 1984. Deformation microfabric development in chalcopyrite in fault zones, Mt. Lyell, Tasmania. *J. Struct. Geol.* **6**, 167–182.

Culshaw, N. G., Davidson, A. & Nadeau, L. 1983. Structural subdivisions of the Grenville Province in the Parry Sound–Algonquin Region, Ontario. In: *Current Research, Part B, Geol. Surv. Pap. Can.* **83-1B**, 243–252.

Culshaw, N. G. & Fyson, W. F. 1984. Quartz Ribbons in high grade granite gneiss: Modifications of dynamically formed quartz *c*-axis preferred orientation by oriented grain growth. *J. Struct. Geol.* **6**, 663–668.

Doherty, R. D. 1974. The deformed state and nucleation of recrystallization. *Metal Sci. J.* **8**, 132–142.

Dillamore, I. L., Morros, P. L., Smith, C. J. E. & Hutchinson, W. B. 1972. Transition bands and recrystallization in metals. *Proc. R. Soc. Lond.* **A 329**, 405–420.

Etheridge, M. A. & Hobbs, B. E. 1974. Chemical and deformational controls on recrystallization of mica. *Contr. Miner. Petrol.* **43**, 111–124.

Hanmer, S. K. & Ciesielski, A. 1984. A structural reconnaissance of the northwest boundary of the Central metasedimentary Belt, Grenville Province, Ontario and Quebec, In: *Current Research, Part B, Geol. Surv. Pap. Can.* **84-1B**, 121–131.

Hobbs, B. E. 1968. Recrystallization of single crystals of quartz. *Tectonophysics* **6**, 353–401.

Inokuti, Y. & Doherty, R. D. 1978. Transmission Kossel study of the structure of compressed iron and its recrystallization behaviour. *Acta Metall.* **26**, 61–80.

Lister, G. S., Paterson, M. S. & Hobbs, B. E. 1978. The simulation of fabric development in plastic development and its application to quartzite: The model. *Tectonophysics* **45**, 107–158.

Lister, G. S. & Paterson, M. S. 1979. The simulation of fabric development during plastic deformation and its application to quartzite fabric transitions. *J. Struct. Geol.* **1**, 99–115.

Lister, G. S. & Hobbs, B. E. 1980. The simulation of fabric development during plastic deformation and its application to quartzite: the influence of deformation history. *J. Struct. Geol.* **23**, 355–370.

Lister, G. S. & Snoke, A. W. 1984. *S–C* mylonites. *J. Struct. Geol.* **6**, 617–638.

McClay, K. R. & Atkinson, B. K. 1977. Experimentally induced kinking and annealing of single crystals of galena. *Tectonophysics* **39**, 175–189.

Means, W. D. 1981. The concept of steady-state foliation. *Tectonophysics* **78**, 179–199.

Means, W. D. 1983. Microstructure and micromotion in crystallization flow of octachloropropane: a first look. *Geol. Rdsch.* **72**, 511–528.

Mitra, S. 1976. A quantitative study of deformation mechanisms and finite strain in quartzites. *Contrib. Miner. Petrol.* **59**, 203–226.

Mitra, S. & Tullis, J. 1979. A comparison of intracrystalline deformation in naturally and experimentally deformed quartzites. *Tectonophysics* **53**, T21–27.

Poirier, J. P. & Guillopé, M. 1979. Deformation induced recrystallization of minerals. *Bull. Minéral.* **102**, 67–74.

Schmid, S. M. 1983. Microfabric studies as indicators of deformation mechanisms and flow laws operative in mountain building. In: *Mountain Building Processes* (edited by Hsu, K. J.). Academic Press, London, 96–110.

Sellars, C. M. 1978. Recrystallization of metals during hot deformation. *Phil. Trans. R. Soc. Ser. A* **288**, 147–158.

Tungatt, P. D. & Humphreys, F. J. 1981. An *in-situ* optical investigation of the deformation behaviour of sodium nitrate—an analogue for calcite. *Tectonophysics* **78**, 661–675.

Walter, J. L. & Koch, E. F. 1963. Structures and recrystallization of deformed (100)(001)-oriented crystals of high-purity silicon–iron. *Acta Metall.* **11**, 923–938.

White, S. 1976. The effects of strain on microstructures, fabric, and deformation mechanisms in quartzites. *Phil. Trans. R. Soc. Ser. A* **283**, 69–86.

White, S. 1977. Geological significance of recovery and recrystallization in quartz. *Tectonophysics* **39**, 143–170.